Electronic Supplementary Material (ESI) for Materials Horizons.

Supporting Information for

Rationalizing Energy Level Alignment by Characterizing Lewis Acid/Base and Ionic Interactions at Printable Semiconductor/Ionic Liquid Interfaces

Linze Du Hill,[a] Michel De Keersmaecker,[a,b] Adam E. Colbert,[c] Joshua W. Hill,[a] Diogenes Placencia,[c] Janice E. Boercker,[c] Neal R. Armstrong,[b] and Erin L. Ratcliff[a,b,d]*

[a] *Department of Chemical and Environmental Engineering, University of Arizona, 1133 E. James E. Rogers Way, Tucson, AZ 85721 USA.*
[b] *Department of Chemistry and Biochemistry, University of Arizona, 1306 E. University Blvd., Tucson, AZ 85721 USA.*
[c] *U.S. Naval Research Laboratory, 4555 Overlook Ave SW, Washington, D.C. 20375, USA.*
[d] *Department of Materials Science and Engineering, University of Arizona, 1235 E. James E. Rogers Way, Tucson, AZ 85721 USA*

Table of Contents:

1. Materials and methods

Sample preparation

Substrates. Template-stripped atomically clean Au foil (5.00 mm × 5.00 mm, Goodfellow, thickness 0.50 mm, high purity 99.999%) was sputter-cleaned (1 hr, 5.00 kV × 8.0 A) before using and verified to be clean by both XPS and UPS. Indium tin oxide (ITO)-coated glass substrates (1.00 × 1.00 cm, Colorado Concept Coatings LLC, ITO 9-15 Ω/sq, thickness 1200-1600 Å) were successively sonicated with Triton X-100 (Sigma, laboratory grade) diluted with ultrapure water, anhydrous ethanol (denatured, VWR, biotechnology grade), acetone (LabChem, 100%), and isopropanol (Fisher Chemical, ≥99.5%) each for 10 mins. All cleaned substrates were stored in isopropanol and dried with N_2 prior to film deposition.

P3HT films. P3HT films were spin-coated (Laurell Technologies Corporation, model WS-650MZ-23NPPB) at 1000 rpm for 1 min using a 10 mg/mL of poly(3-hexylthiophene) (P3HT, Rieke Metals, MW: 48 kg/mol) dissolved in dichlorobenzene (Honeywell, >99%). Subsequently, all polymer films were annealed at 120 °C for 12 mins. The polymer solutions were prepared and kept on a hot plate at 80 °C before spin coated.

NiO_x films. A solution of ethylene glycol (10 mL, Fisher Chemical), ethylene diamine (0.87 mL, Alfa Aesar) and nickel formate (1 g, Alfa Aesar) was heated and stirred until full dissolution was apparent. The solution was filtered (0.45 μm) twice, spin coated (5000 rpm, 1 min) on UV-ozone (10 mins, UVO-Cleaner, Jelight Company) cleaned ITO and annealed (250 °C, 1 hr) to make NiO_x films.

PbS nanocrystal QD synthesis and film preparation. The synthesis of PbS nanocrystals followed the procedure developed by Hines and Scholes, [1] and was performed under inert conditions using standard Schlenk techniques. 1-octadecene (ODE-Sigma Aldrich) was dried and degassed by heating to 110 °C under vacuum for 1 hour, then hexamethyl disilathiane (TMS-Sigma Aldrich) was added to create a stock solution of 151 mM TMS in ODE. In a typical synthesis, 0.36 mg lead oxide (PbO- Sigma Aldrich), 4.8 g oleic acid (OA-Sigma Aldrich) and 8.5 g of ODE were mixed in a 50 mL three neck flask and heated to 110 °C under vacuum for 60 minutes to create Pb(oleate)$_2$. The flask was purged with Ar and heated to an injection temperature between 130 °C. Next, 5 mL of TMS stock solution was injected into the Pb(oleate)$_2$ solution instantly turning the color black. After several minutes, the reaction was cooled by placing the flask in liquid nitrogen, followed by transferring into a nitrogen-purged glovebox. To separate the QDs from unreacted reagents and byproducts, several iterations of an acetonitrile/toluene workup, in conjunction with centrifugation, was conducted. The precipitated QDs formed a black solid at the bottom of the centrifuge vial and the supernatant was removed by decanting. The nanocrystals were dried with a nitrogen stream, followed by storage in a glove box. Substrates of 1 cm × 1 cm size were scrubbed with 10% Triton X-100 (Sigma-Aldrich), followed by sonication in 10% Triton X-100 (15 min), nanopure water (5 min), and absolute ethanol (15 min). The PbS nanocrystals were dispersed in n-heptane at a concentration of 20 mg/mL and deposited via spin coating at 2000 rpm. Ligand exchange was performed by soaking the film surface with PbI$_2$ (10 mM in DMF) for 90 seconds then spinning dry, followed by two subsequent rinses with DMF to remove residual ligand, and a final rinse with acetonitrile to remove residual DMF and yield a dry surface.[2] A total of five layers were deposited to achieve a final film thickness of approximately 100 nm.

MAPbI$_3$ films. The recipe for the formation of the perovskite MAPbI$_3$ has been published recently.[3] Briefly, ca. 324 mg PbI$_2$, and ca. 102 mg of methylammonium iodide (MAI) were transferred to a hot 2-dram vial (stored at 150 °C in an oven to minimize water content) with a micro stir bar and then immediately loaded into a N_2 glovebox. Within the N_2 glovebox, 512 µL of DMF and 128 µL of DMSO were added to the vial (generating solution concentrations of ca. 1:1 M for MAI:PbI_2, respectively), this precursor solution was stirred at 70 ˚C for 20 minutes. The yellow solution was then allowed to cool to room temperature and filtered with a 0.25 µm PTFE syringe filter. The precursor solution was dispensed onto the cleaned ITO substrates (30 µL) at room temperature and then spin-cast at 1000 RPM for 10 seconds (6000 acceleration) followed immediately by 6000 RPM for 20 seconds (6000 acceleration). With five seconds remaining on the spin-coating cycle, 100 µL of chlorobenzene (anti-solvent) was added to the film in a clean dispensing motion as close to the center of the spinning film as possible. All $MAPbI_3$ films were incubated for 1 minute at room temperature in a plastic petri dish with a plastic lid before being transferred to a hot plate for 60 minutes at 100 ˚C as the final thermal annealing step inside the N_2 glovebox. This 1-minute incubation time, followed by the annealing step, ensures conversion to the perovskite product, avoiding excess PbI_2 formation. Glovebox atmosphere circulation (i.e., over an internal purifying catalyst) was kept off throughout the film processing steps described above. After each day of experiments, the glovebox atmosphere was purged for ca. 20 minutes before turning back on the purifier circulation (i.e., until the next experiments involving film processing). $MAPbI_3$ films are kept in the N_2 glovebox until loading into the vacuum chamber for deposition.

Photoelectron spectroscopy

XPS and UPS measurements were performed with a Kratos Axis Ultra X-ray photoelectron spectrometer. XPS used a monochromatic Al Kα source (1486.6 eV) at a base pressure of 5.0×10^{-9} Torr. The operating voltage and current for the source are 15 kV and 10 mA, respectively. Photoelectrons were collected in a hemispherical analyzer and detected with a multichannel array. A 20.00 eV pass energy and a dwell time of 100 ms was used for all element specific spectral acquisitions. The step size for the survey scan was 1.00 eV and for high-resolution regions was 0.02 eV. Resulting XPS spectra were first baseline corrected using a Shirley background in Fityk and then fit using a SplitVoigt peak shape. Ultraviolet photoelectron spectroscopy (UPS) used He

I excitation at 21.22 eV. For UPS measurements the sample is biased at -10.00 V to enhance the yield of electrons at the low kinetic energy edge (LKE). An Ar sputter-etched, atomically clean gold sample was characterized before each analysis run to establish the Fermi edge of the spectrometer. A resolution of 0.06 eV was determined from the Fermi edge.

XPS fitting description of [EMIM$^+$][TFSI$^-$] core levels

The C 1s core levels were fit with five peaks in accordance with a previously described chemical model,[4] using the labeled carbons (C1-C5) in the schematic in Figure S1 of the anion and cation. The binding energy of trace C contamination is 285.0 eV and can be readily observed with no ionic liquid coverage. This peak overlaps with the methyl group (C1) at the end of the ethyl group of [EMIM$^+$] is 284.9 eV at the coverage of 2.0 ML and 3.0 ML, which is shifted 0.2 eV at 4.0 ML and 5.0 ML coverages. The peak (C2) is located at 286.2-286.4 eV associated with two methyl groups ($-CH_3$, $-CH_2-$) directly bonded to the nitrogen of imidazolium. The peak (C3) is associated with carbon from N−C=C−N at 286.8-287.0 eV, with the same area as (C2). The peak (C4) is located at higher binding energy 287.4-287.6 eV is assigned as the N-C=N of imidazolium and the peak area is half of C2 and C3 peaks. Overall, the binding energy was variable from 0.0 ML to 5.0 ML in the range of ± 0.1 eV. Lastly, the anionic trifluoromethyl carbon peak (C5) is observed at 292.7-292.9 eV, which is associated with the CF_3 groups of the [TFSI$^-$] anion.

In addition to C 1s contributions from S 2p, F 1s and O 1s signals could also be observed for the bistriflimide anion. For S 2p, the area ratio of S $2p_{3/2}$ and S $2p_{1/2}$ was kept at 2:1 respectively in accordance with spin-orbit coupling with a constrained full-width half maximum (FWHM) of 1.0 – 1.1 eV for each peak. The peaks are located at S $2p_{3/2}$ ~168.9 eV and S $2p_{1/2}$ ~170.1 eV arise from bistriflimide. The F 1s is fitted with a single peak at 688.8 eV with a FWHM of 1.7 eV. The

O 1s fitted with the solvent contamination (531.9 eV) and the sulfonyl O (~532.5 eV). N 1s fitting is described in the main text.

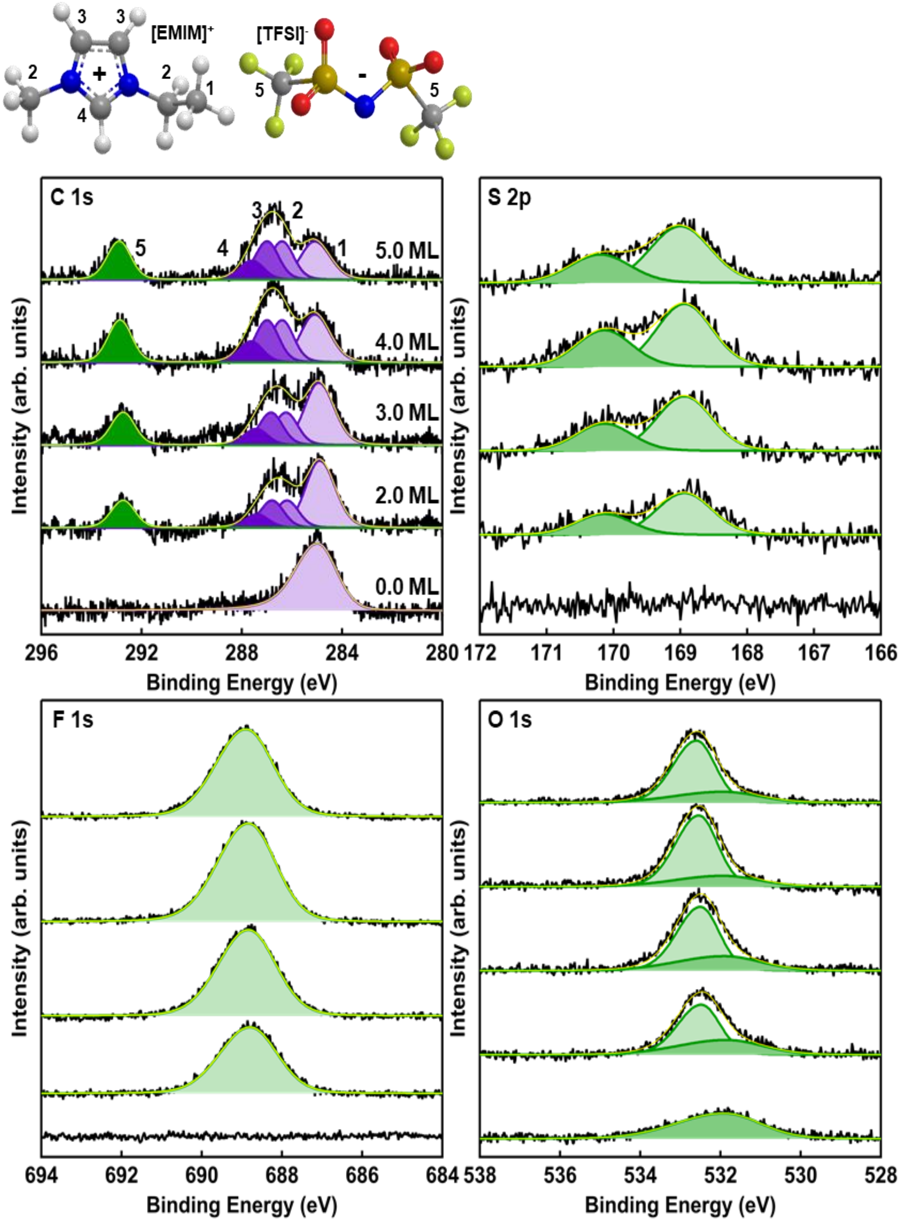

Figure S1. XPS spectra for 0.0, 2.0, 3.0, 4.0, and 5.0 equivalent monolayer coverages of [EMIM$^+$][TFSI$^-$] on Au substrates. The molecular structure of [EMIM$^+$][TFSI$^-$] is located on the top of XPS data (N atoms: blue balls, C atoms: grey balls, H atoms: white balls, S atoms: dark yellow balls, O atoms: red balls, and F atoms: fluorescence yellow balls). The black line is the collected data, and the yellow line is the add-in fitting data.

2. Additional XPS data for [EMIM$^+$] [TFSI$^-$] on Au

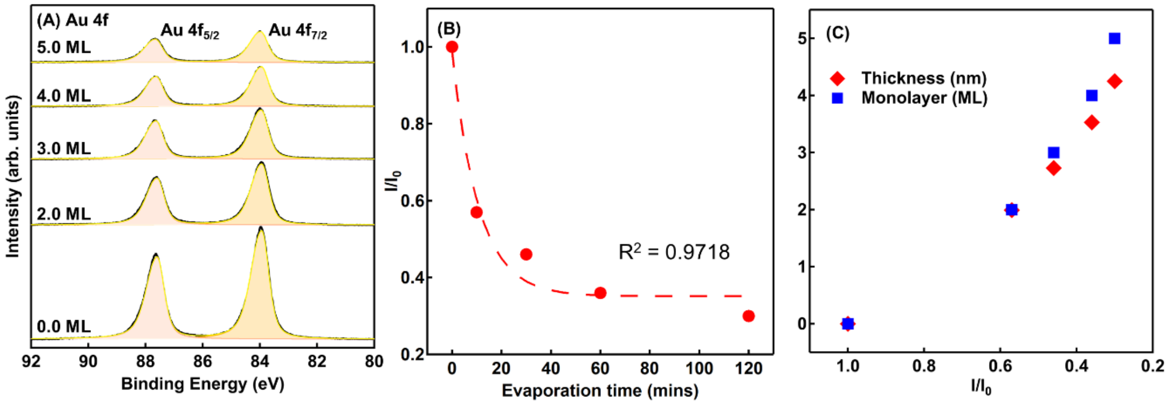

Figure S2. (A) Au 4f spectra for 0.0, 2.0, 3.0, 4.0, and 5.0 ML of [EMIM$^+$][TFSI$^-$]/Au. (B) The normalized area of the Au 4f$_{7/2}$ peak showed a single exponential decay with increasing thickness of the IL layer, allowing for an estimate of the thickness of these layers (C) according to: **Thickness = -ln(I/I_0)** × cos (0°**)** × **3.5nm**) assuming an inelastic mean free path of 3.5 nm.[5] Data in the right-hand plot compares both the estimated thickness and the thickness predicted per monolayer of [EMIM][TFSI]. See also Table S1 below.

Table S1. Evaporation time (mins) of [EMIM$^+$][TFSI$^-$], the fitting area of Au 4f, the area ratio, the calculated thickness, and the estimated monolayers of [EMIM$^+$][TFSI$^-$] are listed in the Table. The fitting area of Au 4f was used in the estimation of the thickness and monolayers of [EMIM$^+$][TFSI$^-$] by using the area ratio as indicated in Fig. S2.

Evaporation Time (mins)	XPS Au Area	I/I_0	Thickness (nm)	ML
0	42516	1.00	0.00	0.0
10	24053	0.57	1.99	2.0
30	19472	0.46	2.73	3.0
60	15487	0.36	3.53	4.0
120	12618	0.30	4.25	5.0

Table S2. Work function (eV) and ionization potential (eV) with standard deviation are listed and collected from UPS on the different coverages (0.0, 2.0, 3.0, 4.0, and 5.0 ML) of [EMIM$^+$][TFSI$^-$]/Au.

Coverage (ML)	Work function (eV)	Ionization potential (eV)
0.0	- 4.9 ± 0.01	
2.0	- 4.3 ± 0.04	- 7.6 ± 0.08
3.0	- 4.1 ± 0.03	- 8.0 ± 0.08
4.0	- 4.1 ± 0.01	- 8.1 ± 0.03
5.0	- 4.2 ± 0.01	- 8.2 ± 0.02

3. UPS of multilayers [EMIM$^+$][TFSI$^-$]/P3HT, NiO$_x$, PbS and MAPbI$_3$ surfaces

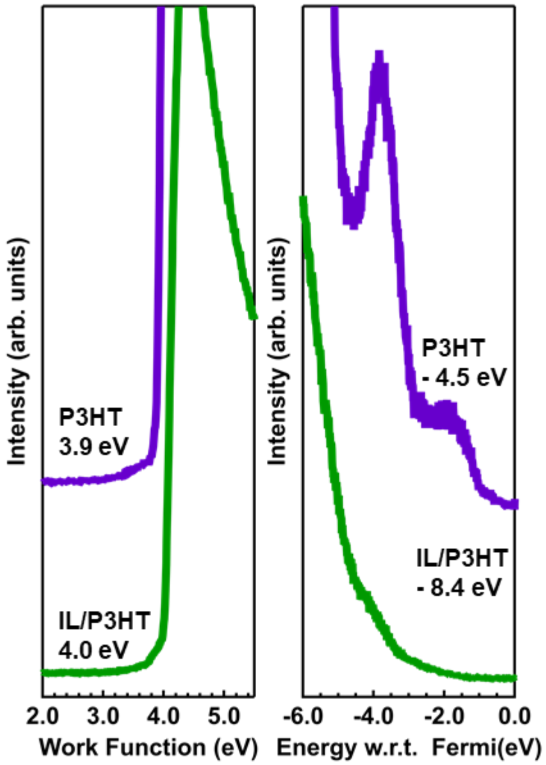

Figure S3. (Left panel) – LKE region and (Right panel) HKE regions of UPS spectra for a prototypical P3HT film and the same film following deposition of the IL. Effective work function and ionization potentials (IP) with respect to vacuum are provided.

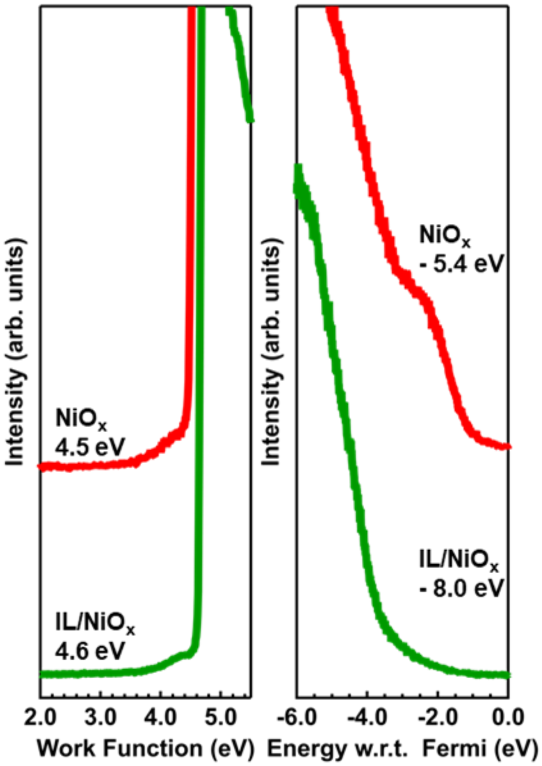

Figure S4. (Left panel) – LKE region and (Right panel) HKE regions of UPS spectra for a prototypical NiO$_x$ film and the same film following deposition of the IL. Effective work function and ionization potentials (IP) with respect to vacuum are provided.

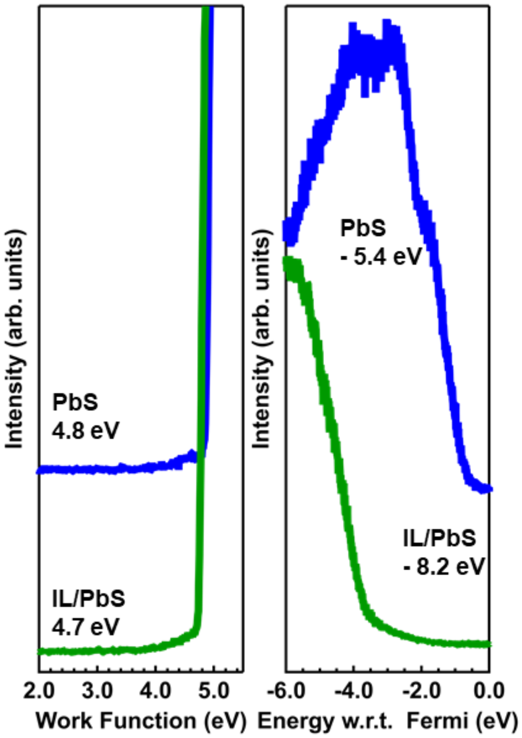

Figure S5. (Left panel) – LKE region and (Right panel) HKE regions of UPS spectra for a prototypical PbI-capped PbS quantum dot film and the same film following deposition of the IL. Effective work function and ionization potentials (IP) with respect to vacuum are provided.

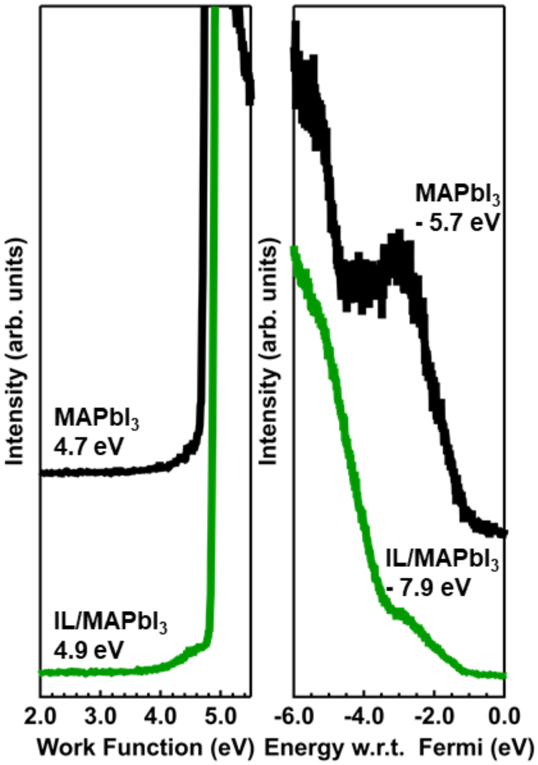

Figure S6. (Left panel) – LKE region and (Right panel) HKE regions of UPS spectra for a prototypical MAPbI$_3$ film and the same film following deposition of the IL. Effective work function and ionization potentials (IP) with respect to vacuum are provided.

4. Conventional semiconductor/electrolyte band bending

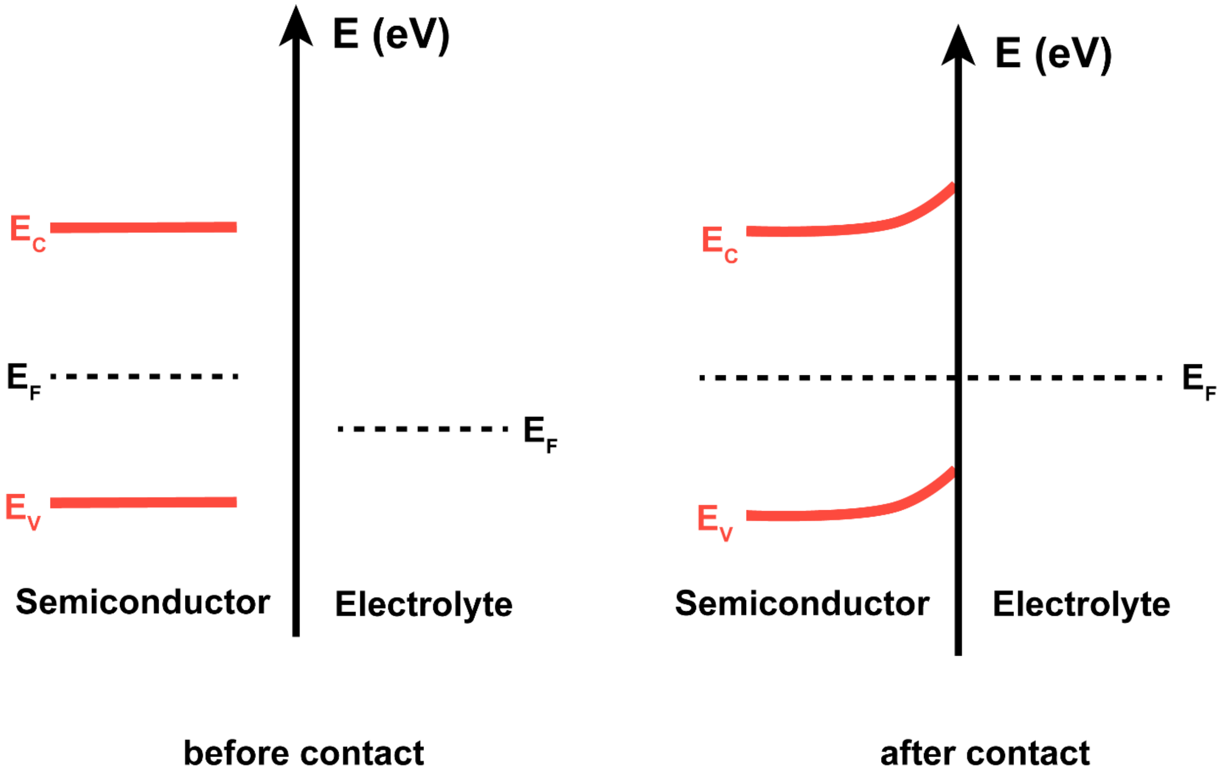

Figure S7. Expected band bending for scenario when the pre-contact work function of semiconductor (e.g. P3HT) is closer to vacuum than work function of IL electrolyte, where electronic equilibration is reached upon heterojunction formation via interfacial charge redistribution and band bending within the near-interface region of the semiconductor. [6] In true band bending, core levels would also bend to same degree as valence and conduction bands.

4. XPS of core level changes of the substrates before and after deposition of the IL [EMIM$^+$][TFSI$^-$] monolayers

Table S3. Spectral assignments for N 1s core levels in Figure 4A. Peak identification, binding energies, binding energy differences between N 1s peaks in the IL cations versus IL anions, full width half maximum (FWHM), and area ratio (anions/cations) are listed from multilayers IL [EMIM$^+$][TFSI$^-$]/various substrates (Au, MAPbI$_3$, PbS, NiO$_x$, and P3HT).

	Peak Identification	**Binding Energy (eV)**	**Δ Binding Energy (eV)**	**FWHM**	**Area Ratio**
IL/Au	bistriflimide anion	399.4		1.2	
	imidazolium cation	402	2.6	1.2	0.5
IL/MAPbI$_3$	bistriflimide anion	399.1		1.2	
	imidazolium cation	401.6	2.5	1.2	0.4
IL/PbS	bistriflimide anion	399.1		1.2	
	imidazolium cation	401.7	2.6	1.2	0.5
IL/NiO$_x$	bistriflimide anion	399.2		1.5	
	imidazolium cation	401.8	2.6	1.5	0.5
IL/P3HT	bistriflimide anion	399.7		1.2	
	imidazolium cation	402.3	2.6	1.2	0.5

Table S4. Spectral assignments for C 1s core levels in Figure 4B. Peak identification, binding energies, and full width half maximum (FWHM) are listed from multilayers IL [EMIM$^+$][TFSI$^-$]/various substrates (Au, MAPbI$_3$, PbS, NiO$_x$, and P3HT).

	Peak Species	**Binding Energy (eV)**	**FWHM**
P3HT	C P3HT	285.0	1.1
IL/P3HT	C P3HT, -CH$_3$	285.1	1.1
	N-CH$_3$, N-CH$_2$-	286.7	1.1
	N−C=C−N	287.3	1.1
	N-C-N of imidazolium	287.9	1.1
	anion trifluoromethyl	293.2	1.1
NiO$_x$	C contamination	284.5	1.1
	C-OH	286.0	1.1
	C=O	287.4	1.1
	O=C-O	288.5	1.1
IL/NiO$_x$	C contamination, -CH$_3$	284.8	1.1
	N-CH$_3$, N-CH$_2$-	286.1	1.1
	N−C=C−N	286.8	1.1
	N-C-N of imidazolium	287.5	1.1
	anionic trifluoromethyl C	292.7	1.1
PbS	C contamination	284.4	1.4
IL/PbS	C contamination, -CH$_3$	284.7	1.1
	N-CH$_3$, N-CH$_2$-	286.0	1.1
	N−C=C−N	286.7	1.1
	N-C-N of imidazolium	287.4	1.1
	anionic trifluoromethyl C	292.6	1.1
MAPbI$_3$	MAPbI$_3$ C-C	285.3	1.1
	MAPbI$_3$ C-N	286.4	1.1
IL/MAPbI$_3$	(IL) -CH$_3$, (MAPbI$_3$) C-C	285.1	1.1
	(IL) N-CH$_3$, N-CH$_2$, (MAPbI$_3$) C-N	286.1	1.1
	N−C=C−N	286.7	1.1
	N-C-N of imidazolium	287.3	1.1
	anionic trifluoromethyl C	292.6	1.1

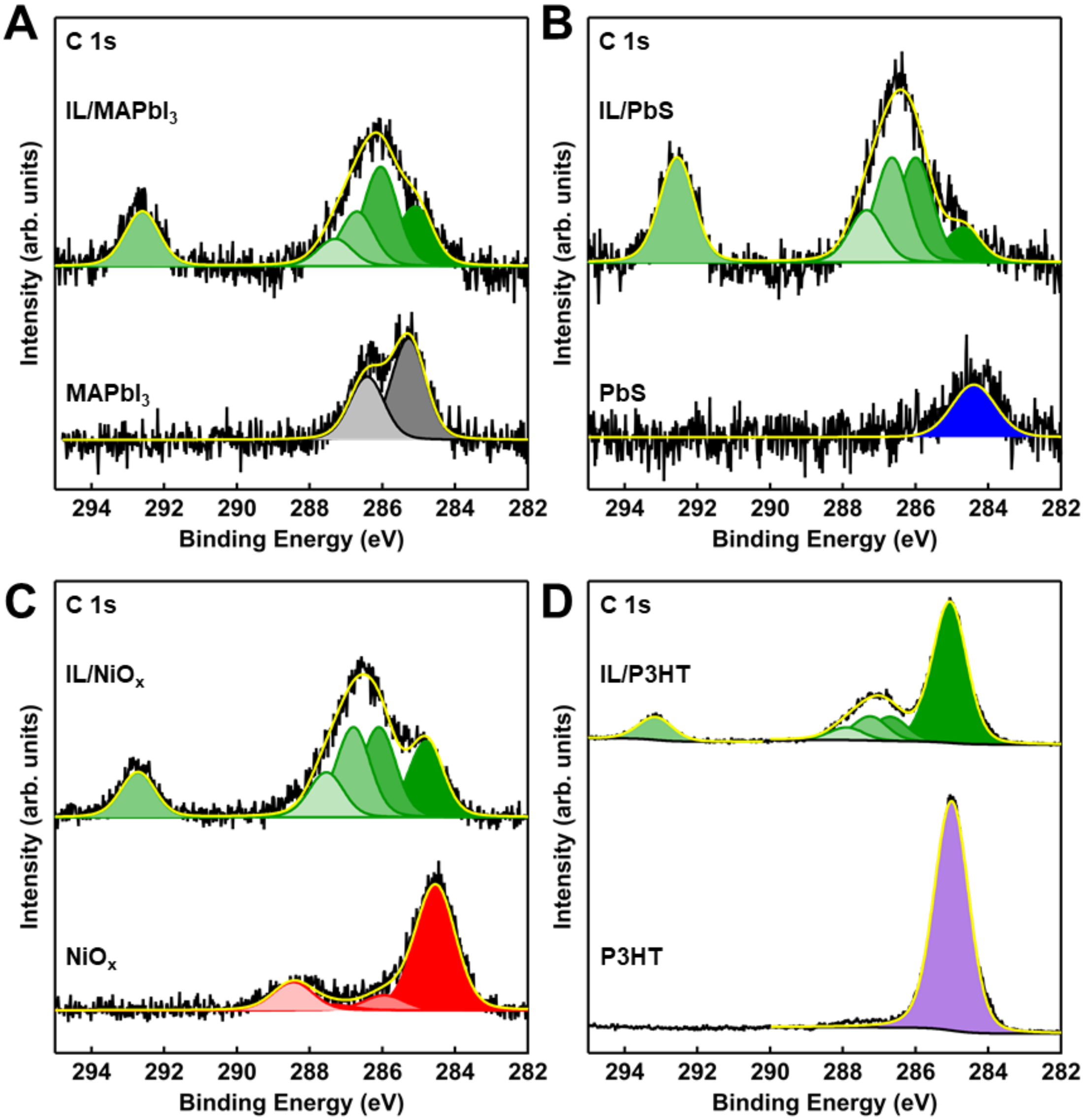

Figure S8. XPS C 1s were collected from multilayers of IL [EMIM$^+$][TFSI$^-$] before and after physical vapor deposition upon A) MAPbI$_3$, B), PbS, C) NiO$_x$, and D) P3HT. The black line is the raw data. The yellow line is the add-in fitting data. The peak fittings of C 1s are displayed in Table S4.

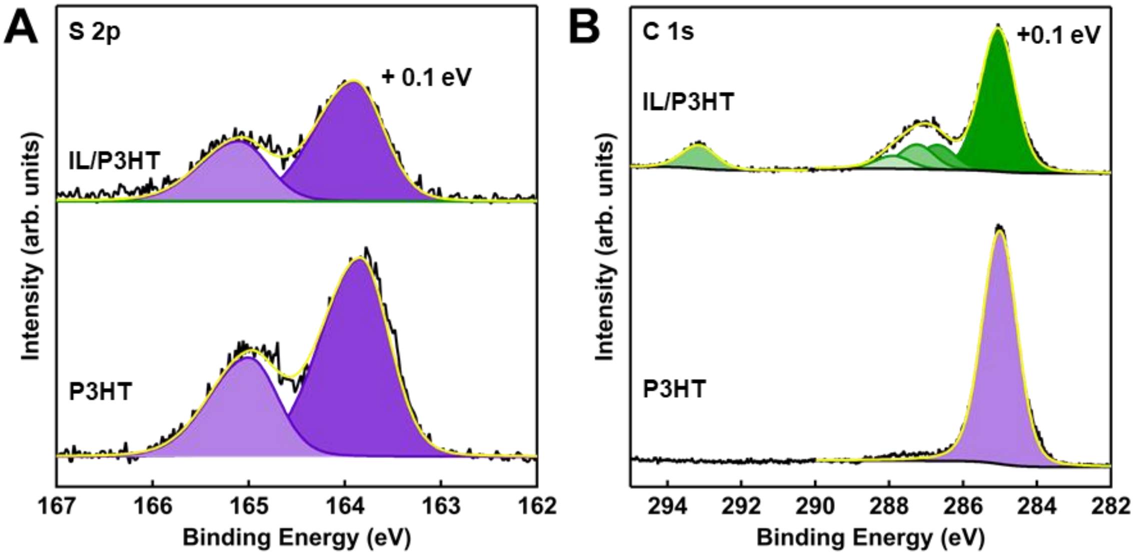

Figure S9. X-ray photoelectron spectroscopy data of the A) S 2p and B) C 1s of as deposited P3HT film before (bottom) and after (top) 3 monolayer depositions of EMIM$^+$/TFSI$^-$. The black line is the raw data, and the yellow line provides the fitting envelope. S 2p data for the TFSI$^-$ anion is not shown to emphasize the minimal shift to the S 2p$_{3/2}$ and S 2p$_{1/2}$ associated with the thiophene unit, constrained to full width half maximums of 1.2 eV and an area ratio of 2:1 in accordance with spin-orbit coupling. Fitting parameters for the C 1s are provided in Table S4.

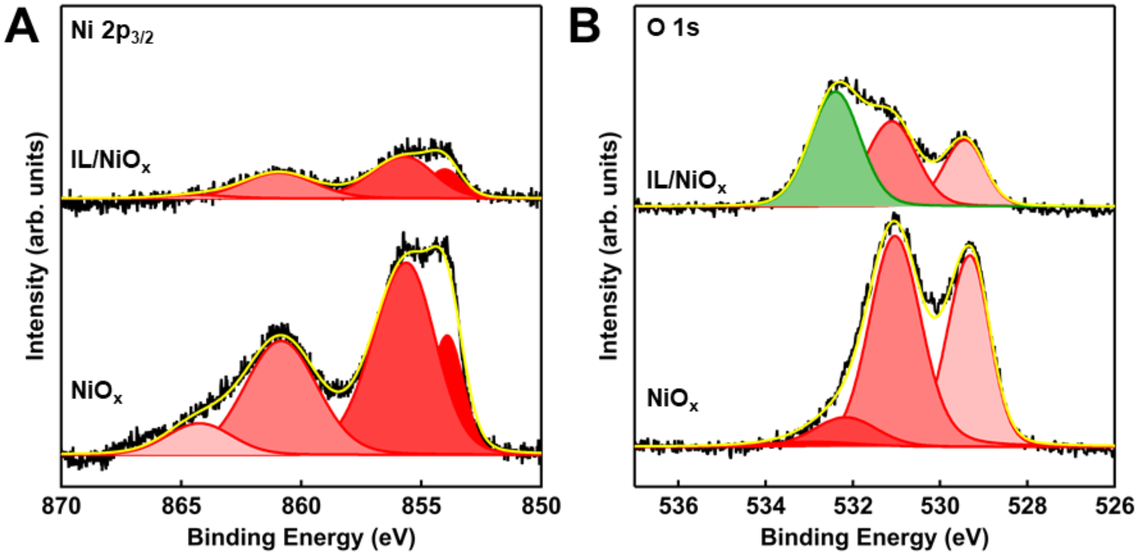

Figure S10. X-ray photoelectron spectroscopy data of A) Ni $2p_{3/2}$ and B) O 1s core levels of the NiO_x film before (bottom) and after (top) 3 monolayers of $EMIM^+$/$TFSI^-$ deposition. Black lines show the raw data and yellow lines show the collective fitting envelop.

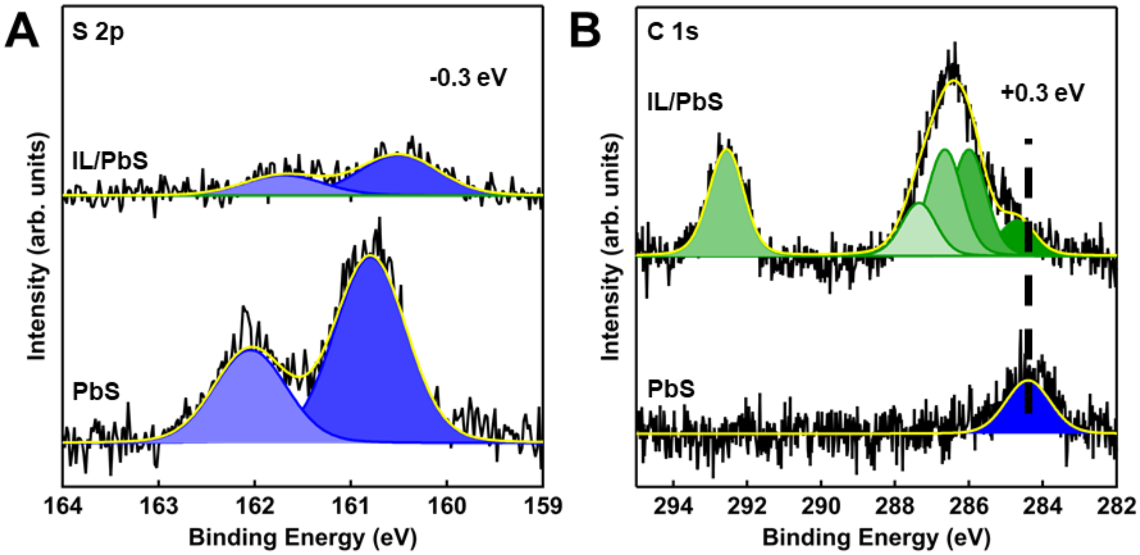

Figure S11. X-ray photoelectron spectroscopy data of A) S 2p and B) C 1s core levels of the PbS quantum dot film before (bottom) and after (top) 3 monolayers of EMIM$^+$/TFSI$^-$ deposition. Black lines show the raw data and yellow lines show the collective fitting envelop. C 1s was fit to EMIM$^+$/TFSI$^-$ model described.

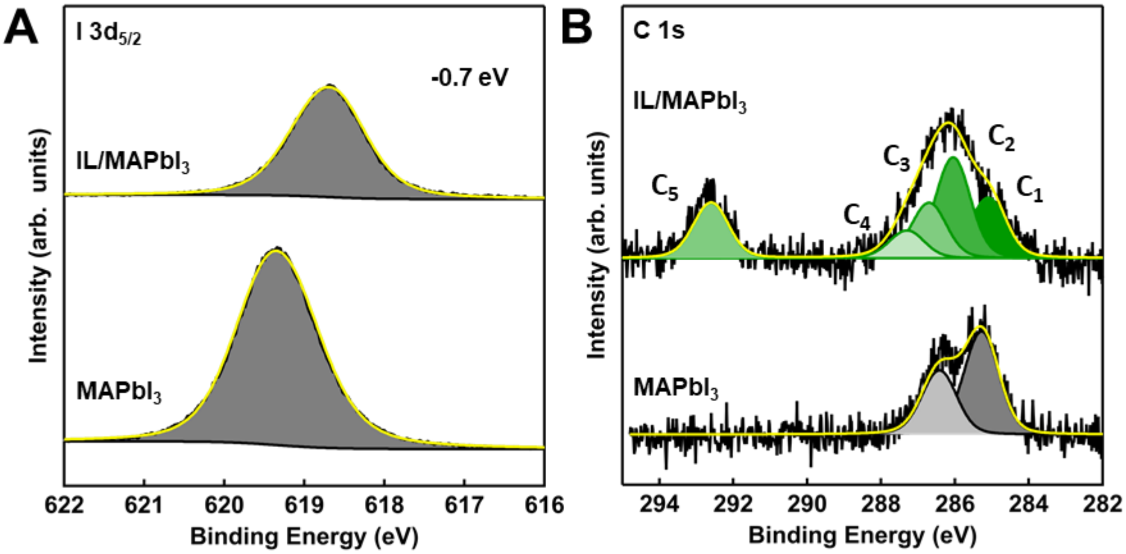

Figure S12. X-ray photoelectron spectroscopy data of A) I $3d_{5/2}$ and B) C 1s core levels on $MAPbI_3$ surface before (bottom) and after 3 monolayers of $EMIM^+/TFSI^-$ deposition. Black lines show the raw data and yellow lines show the collective fitting envelop. We observe a binding energy shift of -0.7 eV in the I $3d_{5/2}$ peak after IL deposition. Peaks in the C 1s spectrum are labeled according to description in the fitting procedure.

XPS S 2p were collected and fitted from [EMIM$^+$][TFSI$^-$]/different printable semiconductors

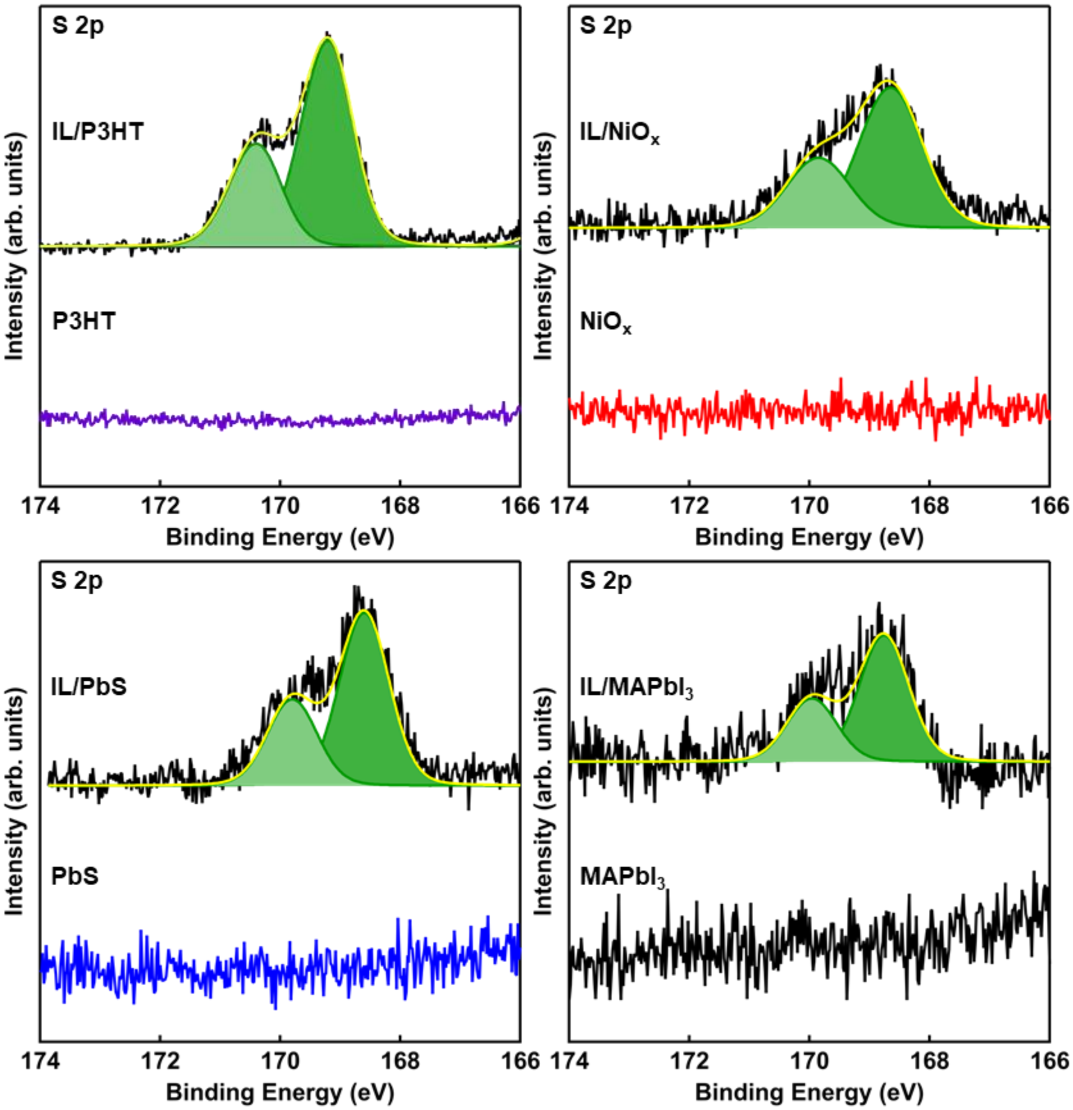

Figure S13. XPS S 2p were collected from multilayers of IL [EMIM][TFSI] before and after physical vapor deposition upon P3HT, NiO$_x$, PbS, and MAPbI$_3$. The black line is the raw data. The yellow line is the add-in fitting data. The peak fittings of S 2p are displayed in Table S5.

Table S5. Peak species, S 2p binding energy, difference binding energy between IL [EMIM][TFSI] S $2p_{3/2}$ and S $2p_{1/2}$, full width half maximum (FWHM), and area ratio (S $2p_{3/2}$ and S $2p_{1/2}$) are listed from multilayers IL [EMIM][TFSI]/various substrates (P3HT, NiO_x, PbS, and $MAPbI_3$).

	Peak Species	**Binding Energy (eV)**	**Δ Binding Energy (eV)**	**FWHM**	**Area Ratio**
IL/P3HT	IL S $2p_{3/2}$	169.2		1.0	
	IL S $2p_{1/2}$	170.4	1.2	1.0	2.0
IL/NiO_x	IL S $2p_{3/2}$	168.7		1.2	
	IL S $2p_{1/2}$	169.9	1.2	1.2	2.0
IL/PbS	IL S $2p_{3/2}$	168.6		1.0	
	IL S $2p_{1/2}$	169.8	1.2	1.0	2.0
IL/$MAPbI_3$	IL S $2p_{3/2}$	168.8		1.0	
	IL S $2p_{1/2}$	170.0	1.2	1.0	2.0

XPS F 1s data from [EMIM$^+$][TFSI$^-$] deposition on different printable semiconductors

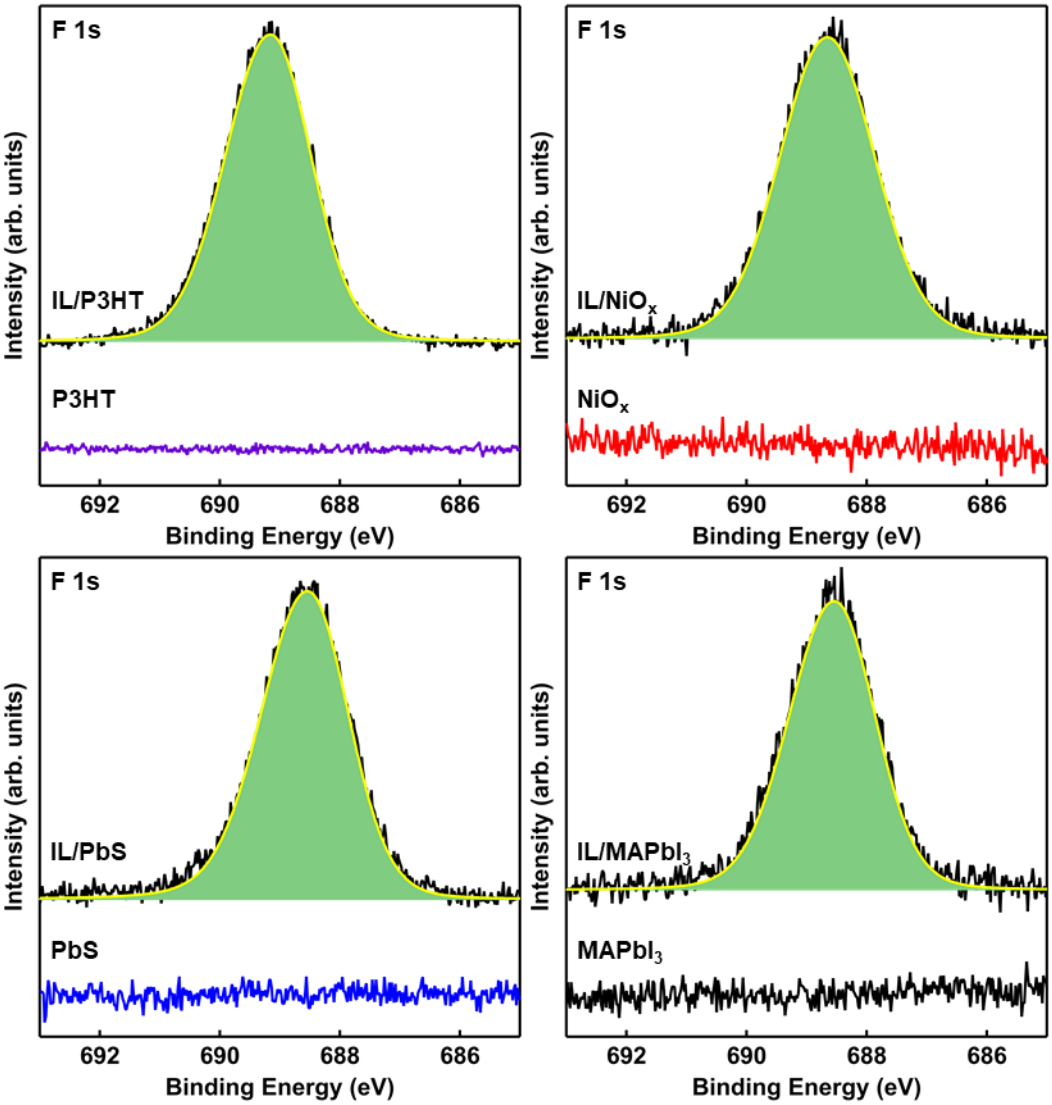

Figure S14. XPS F 1s spectra before and after physical vapor deposition of IL [EMIM][TFSI] on P3HT, NiO$_x$, PbS, and MAPbI$_3$. The black line is the raw data. The yellow line is the add-in fitting data. The peak fittings of F 1s are displayed in Table S6.

Table S6. Peak species, F 1s binding energy and full width half maximum (FWHM) are listed from multilayers IL [EMIM][TFSI]/various substrates (P3HT, NiO_x, PbS, and $MAPbI_3$).

	Peak Species	**Binding Energy (eV)**	**FWHM**
IL/P3HT	anion F	689.2	1.7
IL/NiO_x	anion F	688.7	1.9
IL/PbS	anion F	688.5	1.7
IL/$MAPbI_3$	anion F	688.5	1.7

XPS O 1s data from [EMIM$^+$][TFSI$^-$] deposition on different printable semiconductors

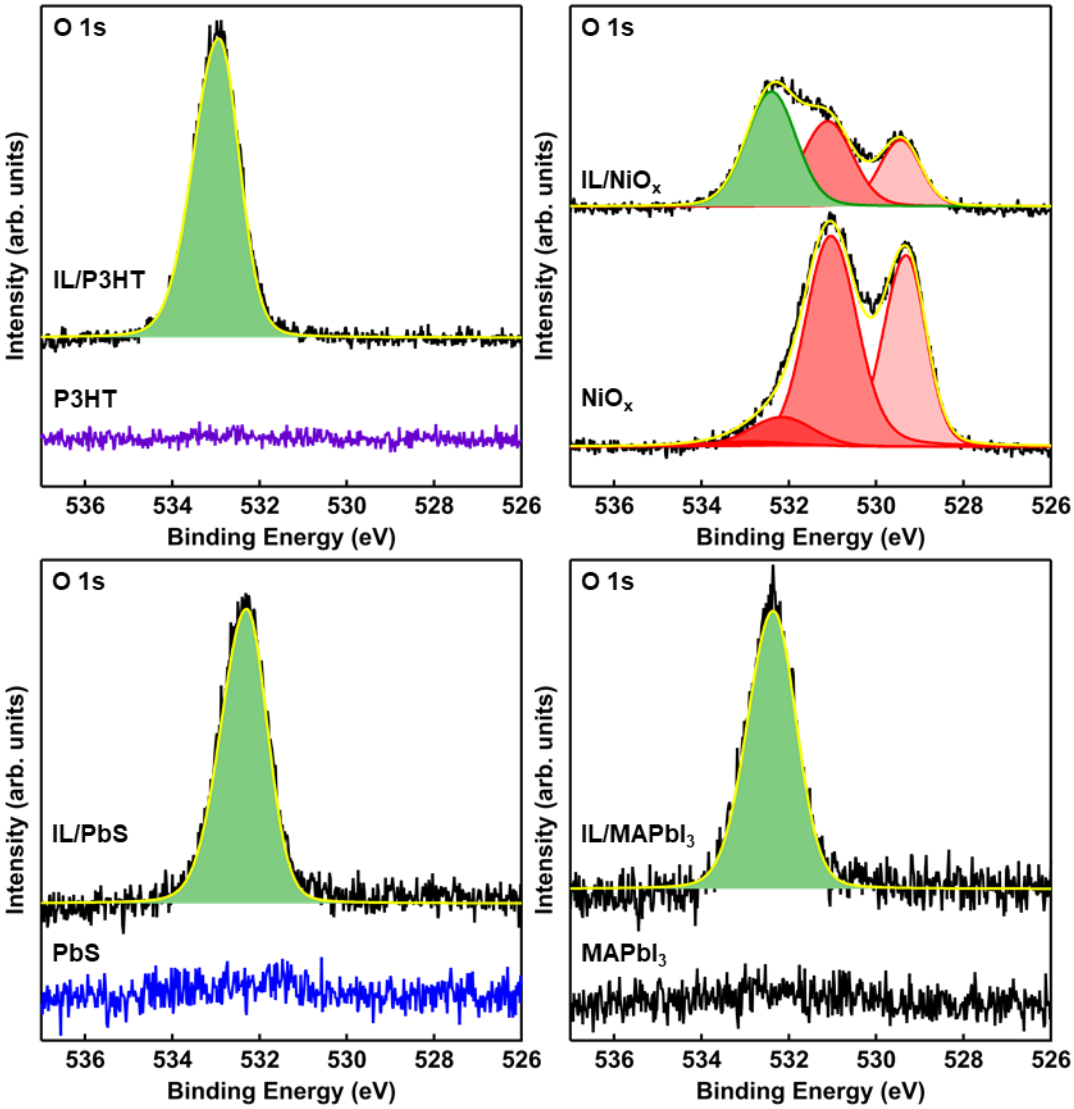

Figure S15. XPS O 1s were collected from multilayers of IL [EMIM][TFSI] before and after physical vapor deposition on P3HT, NiO$_x$, PbS, and MAPbI$_3$. The black line is the raw data. The yellow line is the add-in fitting data. The peak fittings of O 1s are displayed in Table S7.

Table S7. Peak species, O 1s binding energy and full width half maximum (FWHM) are listed from multilayers IL [EMIM][TFSI]/various substrates (P3HT, NiO_x, PbS, and $MAPbI_3$).

	Peak Species	**Binding Energy (eV)**	**FWHM**
IL/P3HT	sulfonyl O	532.9	1.2
NiO_x	NiO-lattice	529.3	1.1
	OH	531.0	1.4
	phys. H_2O	532.2	1.7
IL/NiO_x	NiO-lattice	529.4	1.1
	$Ni(OH)_2$	531.1	1.3
	sulfonyl O	532.4	1.3
IL/PbS	sulfonyl O	532.3	1.3
IL/$MAPbI_3$	sulfonyl O	532.4	1.3

References

1. M. A. Hines and G. D. Scholes, *Advanced Materials*, 2003, **15**, 1844-1849.
2. R. W. Crisp, D. M. Kroupa, A. R. Marshall, E. M. Miller, J. Zhang, M. C. Beard and J. M. Luther, *Scientific Reports*, 2015, **5**, 9945.
3. M. De Keersmaecker, N. R. Armstrong and E. L. Ratcliff, *Energy & Environmental Science*, 2021, **14**, 4840-4846.
4. I. J. Villar-Garcia, E. F. Smith, A. W. Taylor, F. Qiu, K. Lovelock, R. Jones and P. Licence, *Physical Chemistry Chemical Physics*, 2011, **13**, 2797-2808.
5. M. P. Seah and W. A. Dench, *Surface and Interface Analysis*, 1979, **1**, 2-11.
6. R. Memming, in *Semiconductor Electrochemistry*, Wiley-VCH Verlag GmbH, 2015, pp. 169-266.